

## **An Iterative Simultaneous Solution of the Equations of Statistical Equilibrium and Radiative Transfer in the Comoving Frame**

A. Peraiah *Indian Institute of Astrophysics, Bangalore 560034*

Received 1980 June 20; accepted 1980 October 30

**Abstract.** A direct iteration has been performed to obtain a simultaneous solution of the equations of line transfer in an expanding spherically symmetric atmosphere in the comoving frame with statistical equilibrium for a non-LTE, two-level atom. The solution converges in three or four iterations to an accuracy of 1 per cent of the ratio of the population densities of the two levels. As initial values, the upper level population was set equal to zero or to the LTE densities. The final solution on convergence indicates enhanced population of these levels over the initial values assumed. Large velocity gradients enhance this effect whereas large geometrical sizes of the atmospheres tend to reduce it.

*Key words:* statistical equilibrium equation—radiative transfer—comoving frame—iterative solution—velocity gradients

### **1. Introduction**

In solving the transfer equation in spectral lines, several assumptions are made in advance regarding the distributions of velocity, density and other physical variables. These supply the necessary base for a solution of the equation of transfer, no matter how inconsistent the assumptions may be as compared to the real physical situation. Such procedures have been adopted because of several limitations. To obtain the solution of the transfer equation itself is a formidable task. In addition to it, one should understand the extent to which the numerical and physical constraints restrict the usefulness of the solution.

In recent years, there has been a considerable amount of progress in the technique of obtaining a numerical solution of a non-LTE line transfer equation in expanding spherical atmospheres (Simmonneau 1973; Mihalas, Kunasz and Hummer 1975; Peraiah 1979, 1980a) with several assumptions, some of which need not represent the real situation in an extended stellar atmosphere. One should

consider the stellar atmosphere in its entirety to obtain a consistent model, because of the fact that the radiation field and other physical parameters are interdependent. For example the absorption characteristics of the medium could be modified by the stellar radiation field that is incident on the atmospheric material. Again, the new excitation and ionization structure will modify the radiation field which will be noticed in the emergent radiation. Mihalas and Kunasz (1978) attempted to get a simultaneous solution of radiative transfer equation (in the comoving frame) and statistical equilibrium equation using the equivalent two-level atom approach. However, it appears that this takes about 10–15 iterations to obtain convergence of the simultaneous solution. Recently, Kegel (1979) has done extensive calculations towards understanding of the OH masers. He employed a large number of levels in the statistical equation and iterated these with a spatially independent solution of the radiative transport equation. He obtains several interesting results and concludes that the radiative transfer effects are rather important in the study of masers.

In this paper, we try to obtain a simultaneous solution by means of direct iteration of the line transfer equation in comoving frame and with statistical equilibrium equation for a two-level atom.

## 2. Brief description of the computational procedure

The solution of the transfer equation in comoving frame has been described in detail for complete redistribution and for partial frequency redistribution in the framework of discrete space theory (Peraiah 1980 a, b). The transfer equation in the comoving frame for a non-LTE, two-level atom is given by,

$$\begin{aligned} \mu \frac{\partial I(x, \mu, r)}{\partial r} + \frac{1-\mu^2}{r} \frac{\partial I(x, \mu, r)}{\partial \mu} = K_L [\beta + \phi(x)] [S(x, r) - I(x, \mu, r)] \\ + \left\{ (1-\mu^2) \frac{V(r)}{r} + \mu^2 \frac{dV(r)}{dr} \right\} \frac{\partial I(x, \mu, r)}{\partial x}, \end{aligned} \quad (1)$$

and

$$\begin{aligned} -\mu \frac{\partial I(x, -\mu, r)}{\partial r} - \frac{1-\mu^2}{r} \frac{\partial I(x, -\mu, r)}{\partial \mu} = K_L [\beta + \phi(x)] \\ \times [S(x, r) - I(x, -\mu, r)] \\ + \left\{ (1-\mu^2) \frac{V(r)}{r} + \mu^2 \frac{dV(r)}{dr} \right\} \frac{\partial I(x, -\mu, r)}{\partial x}, \end{aligned} \quad (2)$$

where  $I(x, \mu, r)$  is the specific intensity at the radial point  $r$ , making an angle  $\cos^{-1}\mu$  with the radius vector.  $V(r)$  is the gas velocity at  $r$  in terms of mean thermal velocity

units (mtu). The quantity  $x$  is equal to  $(\nu-\nu_0)/\Delta s$  where  $\Delta s$  is a standard frequency interval. The profile function  $\phi(x)$  is normalized such that

$$\int \phi(x) dx = 1. \quad (3)$$

$S(x, \mu, r)$  is the source function given by (Grant and Peraiah 1972)

$$S(x, r) = \frac{\phi(x)}{\beta + \phi(x)} S_L(r) + \frac{\beta}{\beta + \phi(x)} S_C(r), \quad (4)$$

where  $\beta$  is the ratio  $K_C/K_L$  of opacities in the continuum and line per unit interval of  $x$ , and  $S_L(r)$  and  $S_C(r)$  are the line and continuum source functions respectively.  $S_L$  is given in terms of population densities of the two levels

$$S_L(r) = A_{21} N_2(r) / [B_{12} N_1(r) - B_{21} N_2(r)]. \quad (5)$$

The absorption coefficient  $K_L(r)$  at line centre is given by

$$K_L(r) = \frac{h \nu_0}{4\pi \Delta s} (N_1 B_{12} - N_2 B_{21}), \quad (6)$$

where  $A_{21}$ ,  $B_{12}$  and  $B_{21}$  are the Einstein coefficients and  $N_1(r)$  and  $N_2(r)$  are the population densities of the lower and upper levels respectively. The statistical equilibrium equation for the two levels is given by

$$\begin{aligned} N_1 \left[ B_{12} \int_{-\infty}^{+\infty} dx \phi(x) \frac{1}{2} \int_{-1}^{+1} I(\mu) d\mu + C_{12} \right] \\ = N_2 \left[ A_{21} + C_{21} + B_{21} \int_{-\infty}^{+\infty} dx \phi(x) \frac{1}{2} \int_{-1}^{+1} I(\mu) d\mu \right]. \end{aligned} \quad (7)$$

The frequency independent line source function  $S_L(r)$  in equation (5) can also be written as

$$S_L(r) = (1 - \epsilon) \int_{-\infty}^{+\infty} \phi(x) J(x) dx + \epsilon B, \quad (8)$$

where  $B$  is the Planck function and  $\epsilon$  is the probability that a photon is lost by collisional de-excitation in one scattering. This is given by  $\epsilon = C/(C+A_{21})$  where  $C = C_{21}[1 - \exp(-h\nu/kT)]$ .

We are primarily interested in finding out the capabilities of this method in handling iterative problems. We have, therefore, chosen an isothermal atmosphere with  $T_{\text{eff}} = 30,000$  K. The atomic parameters of hydrogen Lyman Alpha line have been

chosen. The inner radius of the atmosphere is set equal to  $10^{12}$  cm. As we are using a velocity law, where the velocity increases linearly with radius, we have adjusted the electron density  $N_e(r)$  and neutral atom density  $N(r)$ , ( $N(r) = N_1(r) + N_2(r)$  where  $N_1(r)$  and  $N_2(r)$  are the neutral atoms in level 1 and 2 respectively) at every radial point such that they always satisfy the equation of continuity. As the velocity increases outwards the optical depth decreases and we have  $dV/dr < 0$ . The number of neutral atoms are calculated by using the Saha equation (Aller 1963)

$$\log \frac{N_1 P_e}{N_0} = -\theta I + 2.5 \log T - 0.48 + \log 2 u_1(T)/u_2(T), \quad (9)$$

where  $I$  is the ionization potential in volts,  $P_e$  is the electron pressure in dynes  $\text{cm}^{-2}$ ,  $\theta$  is equal to  $5040/T$  and  $u$ 's are the partition functions. We have set  $N_e = 10^{14} \text{ cm}^{-3}$ . The rates of collisional excitation and de-excitation are calculated by the relations (Jefferies 1968)

$$C_{12} \simeq 2.7 \times 10^{-10} \alpha_0^{-1.68} \exp(-\alpha_0) T^{-3/2} A_{21} \frac{g_2}{g_1} (I_H/\chi_0)^2 N_e, \quad (10)$$

and

$$C_{21} = 2.7 \times 10^{-10} \alpha_0^{-1.68} T^{-3/2} A_{21} (I_H/\chi_0)^2 N_e, \quad (11)$$

where  $\chi_0$  is the excitation energy  $E_{12}$  and  $\alpha_0 = \chi_0/kT$ .  $I_H$  is the ionization potential of hydrogen. We have considered two cases (1)  $\beta = 0$  and  $\epsilon \ll 1$  and (2)  $\beta \sim \tau_{\text{shell}}^{-1}$  and  $\epsilon \ll 1$ . We have kept  $N_2 = 0$  or its LTE value and the absorption coefficient is calculated by using equation (6) and hence the optical depth in a given shell. With these initial data, equations (1) and (2) are solved to obtain the mean intensities  $J_x$ . These mean intensities  $J_x(r)$  are used to obtain a new set of  $N_1(r)$  and  $N_2(r)$  by solving the statistical equilibrium equation (7) and keeping  $N(r) = N_1(r) + N_2(r)$ . The new absorption coefficient is estimated with the help of equation (6), by which the transfer equations (1) and (2) are solved again. This process has been repeated until the population densities  $N$ 's, at each radial point converge within 1 per cent in two successive iterations.

### 3. Discussion of the results

As we are treating only the statistical equilibrium equation and the equation of radiative transfer, we need several parameters to be specified in advance. We have chosen the quantity  $B/A$  (where  $B$  and  $A$  are the outer and inner radii of the medium) to be 3, 10 and 20. we have used a velocity law

$$V(r) = V_A + \frac{V_B - V_A}{B - A}(r - A), \quad (12)$$

where  $V(r)$ ,  $V_A$  and  $V_B$  are the velocities at  $r$ ,  $A$  and  $B$  respectively.  $V_A$  is set equal to zero and  $V_B$  is set equal to 0, 5, 10, 30, 60 and 100 mtu.

In the first iteration we started with  $N_1(r) = N(r)$  and  $N_2(r) = 0$ . In the second iteration the new values of  $N_1(r)$  and  $N_2(r)$  are employed to calculate the radiation field and this process is continued until convergence is achieved. We have chosen the population density as the criterion for the convergence because the absorption and emission characteristics are dependent on these quantities. The whole medium has been divided into 30 shells of equal geometrical thickness and it is ensured that at all the shell boundaries the quantities  $N_1(r)$  and  $N_2(r)$  in two successive iterations do not differ by more than 1 per cent.

In Figs 1 and 2, we have presented the ratio  $N_2/N_1$  and the line source function calculated by equation (5) with respect to the optical depth in the medium for  $B/A=3$  and 10 respectively. We have set  $\beta = 0$  and  $\epsilon \ll 1$ . The maximum velocities we have used are  $V_B = 0, 5, 10, 30, 60$  mtu. We notice a close similarity between the variation of  $S_L$  and  $N_2/N_1$  with optical depth. At maximum  $\tau$  we have maximum  $N_2/N_1$  and  $S_L$ . The absolute value of  $N_2/N_1$  is less than  $10^{-2}$  whereas for the same temperature the equilibrium value is  $7.8 \times 10^{-2}$ . This solution converged, in three iterations to the same ratio of  $N_2/N_1$  irrespective of the fact

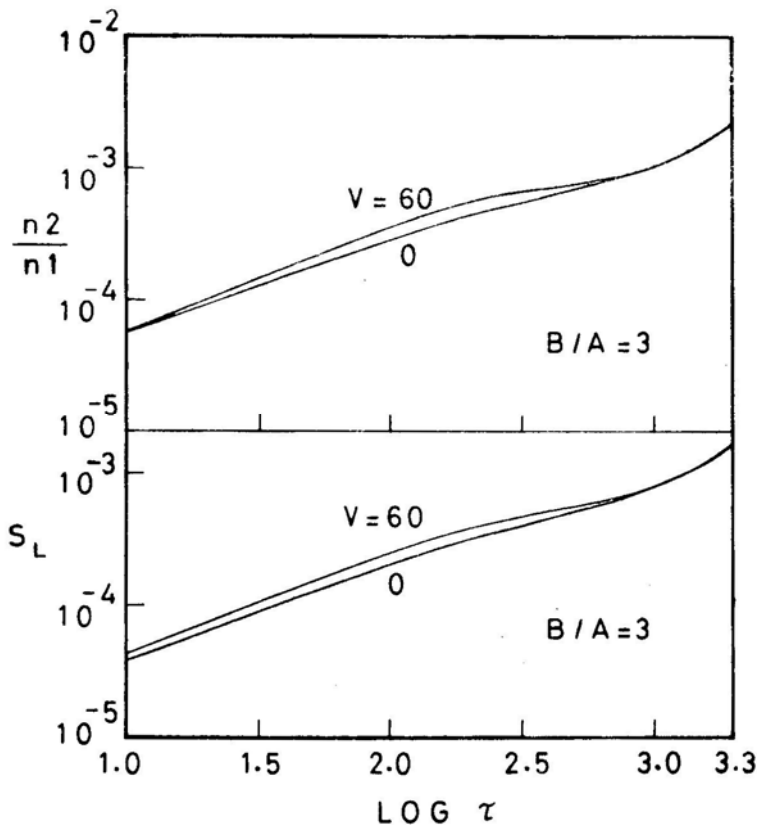


**Figure 1.** The line source functions  $S_L$  and  $N_2/N_1$  are plotted against the optical depth for  $B/A=3$  and  $V_B=0$  and 60.

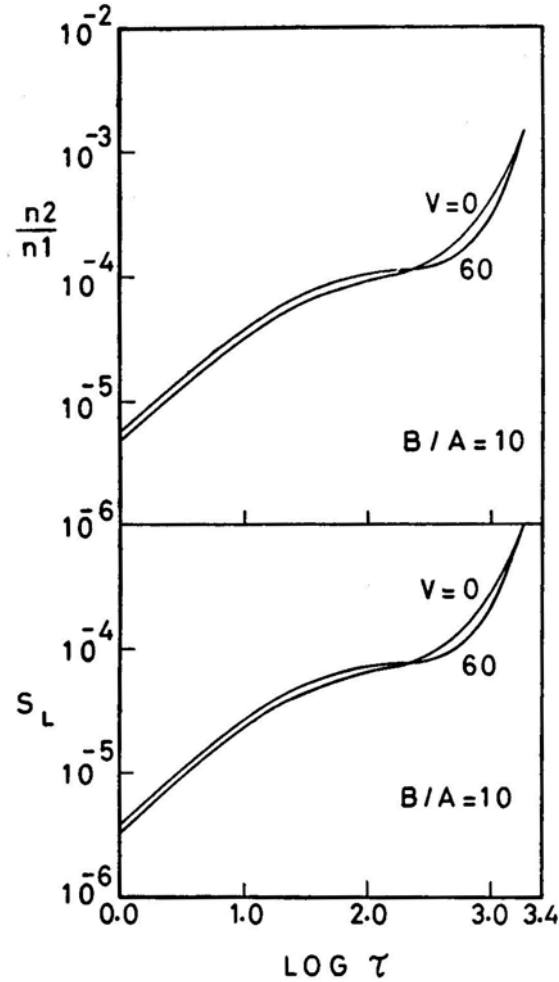


**Figure 2.** The line source functions  $S_L$  and  $N_2/N_1$  are plotted against the optical depth for  $B/A = 10$ .

whether or not the initial  $N_2/N_1$  is zero or the LTE value. The change in the maximum velocities does not seem to have much effect and therefore we have presented only those results that can be clearly seen in the figures. Fig. 3 gives us the flux profiles at infinity. For  $V_B = 0$  (*i.e.* stationary medium) we obtain emission profiles with central absorption. However, when motion is introduced, the central absorption is replaced by emission. This is because of the fact that when more matter moves radially outwards into the side lobes the amount of scattering increases and this enhances the emission in the line (Peraiah 1980b).

In Fig. 4, we have plotted  $\Delta N/N_1$ , where  $\Delta N = N_2 - N_1$ , against the optical depth for  $B/A = 3$  and  $V_B = 0, 5, 30, 60$  and  $100$  mtu. We have set  $\beta = \tau_{\text{shell}}^{-1}$ . Therefore  $\beta$  changes between  $10^{-2}$  and  $10^{-4}$  in the medium. In spite of the fact that we have started the iteration with  $N_2(r) = 0$ , the converged solution shows that  $N_2(r)$  is nearly

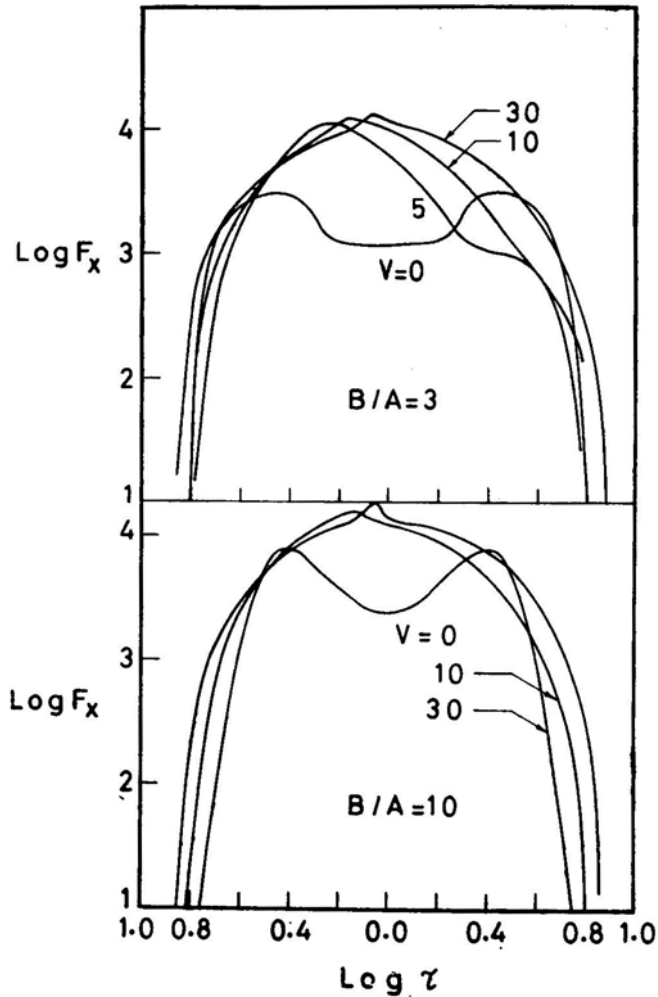


**Figure 3.** Flux profiles at infinity are given corresponding to the source functions given in Figs 1 and 2.

equal to  $N_1(r)$ . At  $\tau = 0$ ,  $N_1 N_1(r) > N_2(r)$  and the quantity  $\Delta N/N_1$  falls off slowly, while at  $\tau = \tau_{\max}$  there is a sharp fall in  $N_2(r)$ . If we compare the results of Fig. 1 with those of Fig. 4, we notice that  $N_2/N_1 \ll (N_2/N_1)_{\text{LTE}}$  in the former case and  $N_2/N_1 \ll (N_2/N_1)_{\text{LTE}}$  in the latter. These differences arise because of the high mean intensities in the medium with  $\beta > 0$ . Results of Fig. 1 represent a medium with scattering whereas the results of Fig. 4 represent the medium with both line emission and scattering. The ratio  $N_2/N_1$  is given by

$$\frac{N_2}{N_1} = \frac{B_{12} \int J_x \phi_x dx + C_{12}}{A_{21} + C_{21} + B_{21} \int J_x \phi_x dx}.$$

In this case,  $C_{12}, C_{21} \ll B_{12}, B_{21}$  and  $A_{21}$ . Therefore,

$$\frac{N_2}{N_1} = \frac{B_{12} \int J_x \phi_x dx}{A_{21} + B_{21} \int J_x \phi_x dx} \tag{13}$$

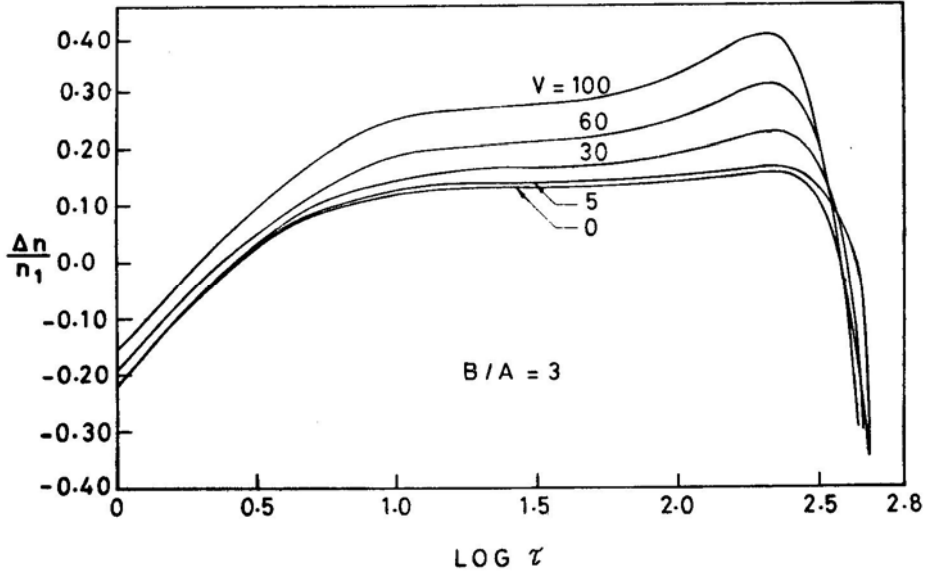


Figure 4.  $\Delta N/N_1$  where  $\Delta N = N_2 - N_1$  are plotted against total optical depth  $\tau$  for  $B/A=3$ .

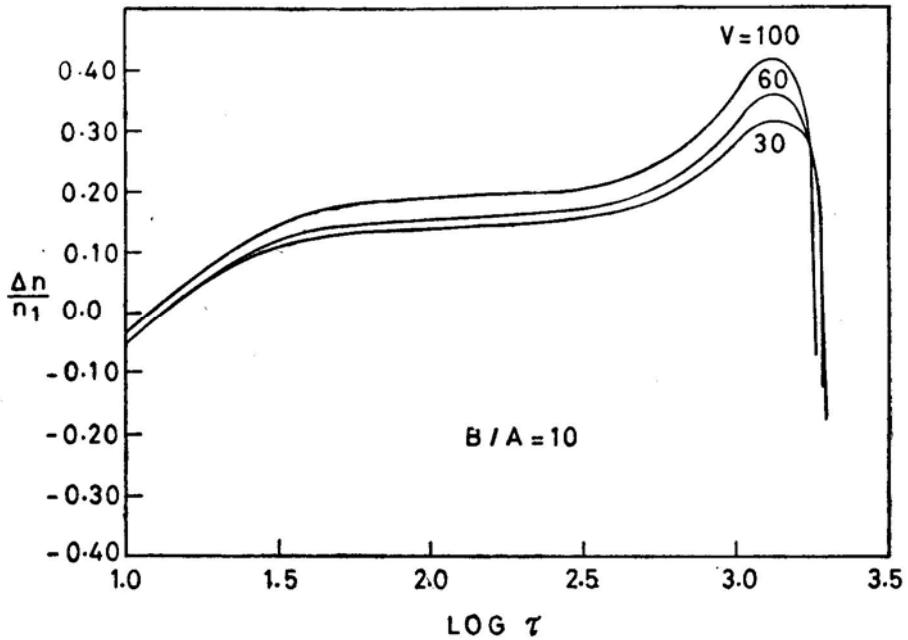


Figure 5.  $\Delta N/N_1$  are given against total  $\tau$  for  $B/A=10$ .

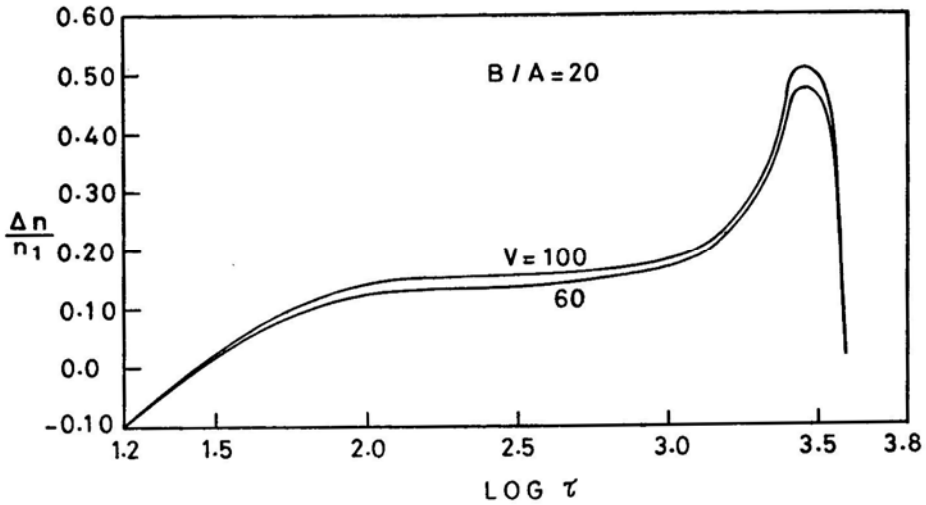


Figure 6.  $\Delta N/N_1$  are given against total  $\tau$  for  $B/A=20$ .

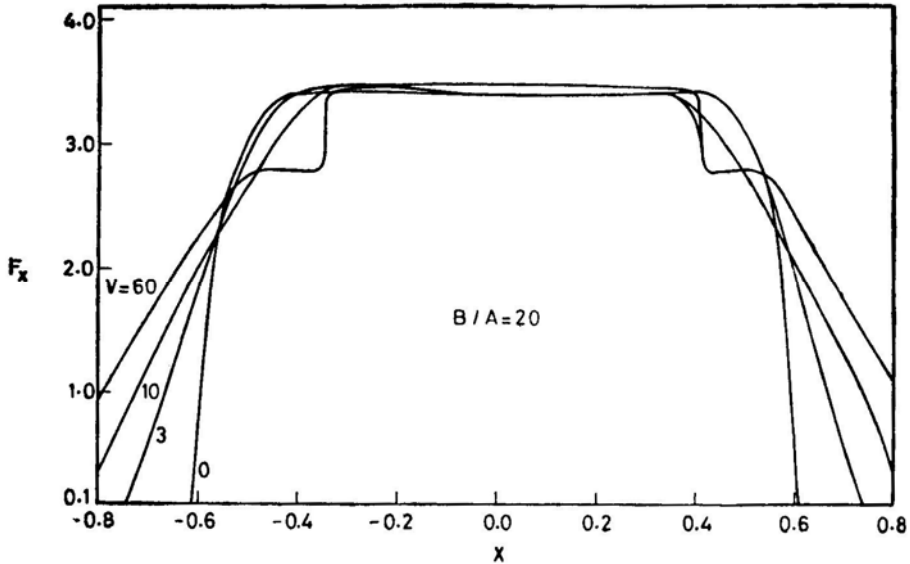


Figure 7. The flux profiles are plotted corresponding to the population density distribution given in Fig. 4. The abscissa is  $Q = X/X_{max}$ .

One can estimate approximately the order of magnitude of  $N_2/N_1$  using equation (13). In both the cases, for hydrogen  $L_\alpha$  line at 30,000K, at some point in the atmosphere, we obtain,  $N_2/N_1 \sim 10^{-4}$  in the first case and  $N_2/N_1 \sim 1$  in the second case. This is so because the mean intensities are reduced considerably in the scattering medium with  $\beta=0$  and  $\epsilon < 1$ , while in the emitting medium with  $\beta > 0$  the mean intensities are much higher.

It is very interesting to notice that as  $|dV/d\tau|$  increases the ratio  $\Delta N/N_1$  increases and this is accentuated at large optical depth. For  $V_B = 100$  mtu of the gas velocity,

the maximum value of  $\Delta N/N_1$  is as great as 0.4. In Figs 5 and 6, we have plotted  $\Delta N/N_1$  for  $B/A=10$  and 20 respectively. One observes immediately that the curves tend to converge for various values of  $|dV/d\tau|$ , and that they become unresolvable graphically until  $V_B=60$  mtu of the gas velocity. The effects of high velocities which we noticed in Fig. 4 seem to be slightly reduced because of high curvature factors. As we are considering a much larger geometrical thickness, other factors being kept constant, the optical depth increases as  $B/A$  increases. We can also notice that the curves become flatter as  $B/A$  increases. In all other respects the results of Figs 2 and 3 are similar to those given in Fig. 1.

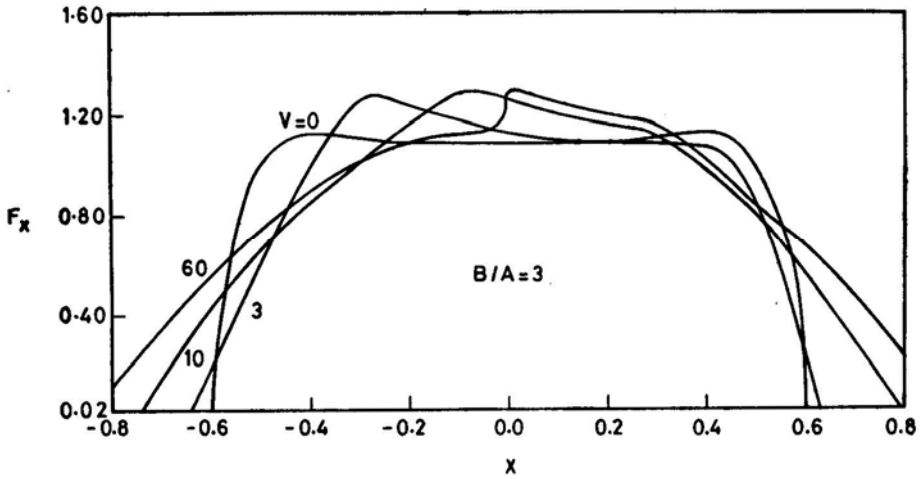


Figure 8. The flux profiles corresponding to the population distribution given in Fig. 5.

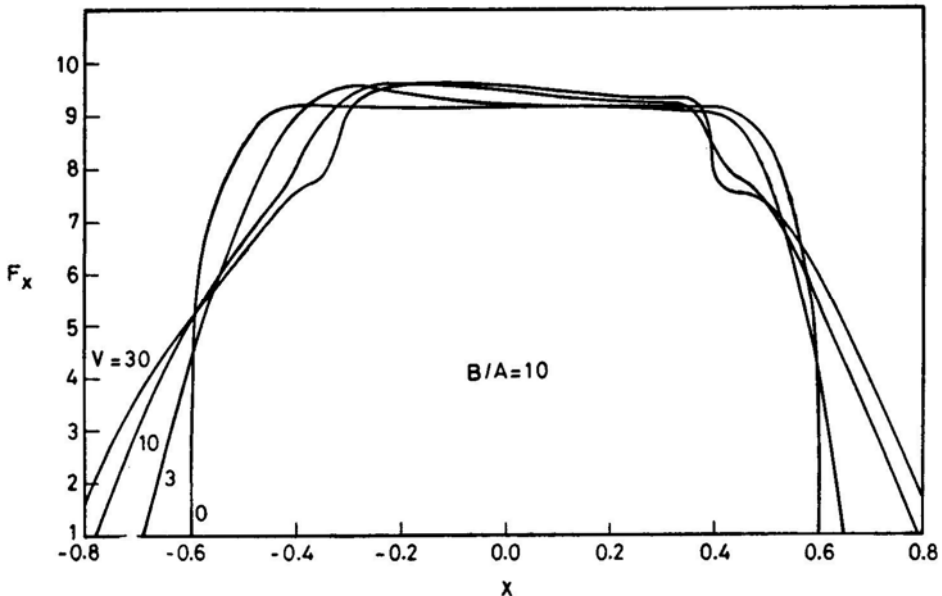


Figure 9. Same as those given in Figs 7 and 8 but corresponding to the population density distribution given in Fig.6.

The line source function  $S_L(r)$  is calculated either from equation (5) or from equation (8) and the total source function is computed from equation (4). The line profiles seen by an observer at infinity are computed by using the total source function (Peraiah 1980b). These are given in Figs 7–9, for  $B/A = 3, 10$  and  $20$  respectively. For stationary medium, symmetric emission emerge for all values of  $B/A$ . However, for small  $|dV/d\tau|$  when  $B/A=3$ , a small amount of asymmetry arises with red emission. For large  $B/A$ 's and  $|dV/d\tau|$  we obtain almost symmetric profiles.

### Acknowledgements

The author would like to thank Prof. Dr. W. H. Kegel, Dr. R. Wehrse and a referee for their useful comments.

### References

- Aller, L. H. 1963, *Astrophysics: The Atmospheres of the Sun and Stars*, 2 edn, Ronald, New York.  
Grant, I. P., Peraiah, A. 1972, *Mon. Not. R. astr. Soc.*, **160**, 239.  
Jefferies, J. 1968, *Spectral Line Formation*, Blaisdel, Waltham.  
Kegel, W. H. 1979, *Astr. Astrophys. Suppl. Ser.*, **38**, 131.  
Mihalas, D., Kunasz, P. B. 1978, *Astrophys. J.*, **219**, 635.  
Mihalas, D., Kunasz, P. B., Hummer, D. G. 1975, *Astrophys. J.*, **202**, 465.  
Peraiah, A. 1979, *Kodaikanal Obs. Bull. Ser. A*, **2**, 115.  
Peraiah, A. 1980a, *Acta Astr.*, (in press).  
Peraiah, A. 1980b, *J. Astrophys. Astr.*, **1**, 3.  
Simmonneau, E. 1973, *Astr. Astrophys.*, **29**, 357.